

Journal of Biomedical Optics

SPIEDigitalLibrary.org/jbo

Effects of pathology dyes on Raman bone spectra

Karen A. Esmonde-White
Francis W. L. Esmonde-White
Michael D. Morris
Blake J. Roessler

Effects of pathology dyes on Raman bone spectra

Karen A. Esmonde-White,^a Francis W. L. Esmonde-White,^b Michael D. Morris,^b and Blake J. Roessler^a

^aUniversity of Michigan Medical School, Department of Internal Medicine, Division of Rheumatology, 1150 W. Medical Center Drive, Ann Arbor, Michigan 48109-0688

^bUniversity of Michigan, Department of Chemistry, Ann Arbor, Michigan 48109

Abstract. We report an overlooked source of artifacts for clinical specimens, where unexpected and normally negligible contaminants can skew the interpretation of results. During an ongoing study of bone fragments from diabetic osteomyelitis, strong Raman signatures were found, which did not correspond with normal bone mineral or matrix. In a bone biopsy from the calcaneus of a patient affected by diabetic osteomyelitis, Raman microspectroscopic analysis revealed regions with both abnormal mineral and degraded collagen in addition to normal bone. Additional bands indicated a pathological material. *Stenotrophomonas maltophilia* was identified in the wound culture by independent microbiologic examination. We initially assigned the unusual bands to xanthomonadin, a bacterial pigment from *S. maltophilia*. However, the same bands were also found more than a year later on a second specimen that had been noticeably contaminated with pathology marking dye. Drop deposition/Raman spectroscopy of commonly used pathology dyes revealed that a blue tissue-marking dye was responsible for the unusual bands in both specimens, even in the first specimen where there was no visible evidence of contamination. © 2013 Society of Photo-Optical Instrumentation Engineers (SPIE) [DOI: 10.1117/1.JBO.18.5.057002]

Keywords: Raman spectroscopy; bacterial pigment; bone; osteomyelitis; pathology dye; bone infection; xanthomonadin; *Stenotrophomonas maltophilia*.

Paper 12813TNRR received Dec. 20, 2012; revised manuscript received Mar. 28, 2013; accepted for publication Apr. 4, 2013; published online May 2, 2013.

1 Introduction

Subtle changes to composition or molecular structure are often the first indications of disease, but these changes cannot be measured by standard clinical or laboratory tests. Raman spectroscopy of bone in disease has received much attention because it can be used to examine these subtle alterations, with a potential for *in vivo* applications.^{1–6} In the course of an ongoing clinical study to characterize bone composition in diabetic osteomyelitis using Raman spectroscopy, a specimen from the University of Michigan (UM) hospital was examined. Raman spectra from this specimen contained strong unusual Raman bands that could not be assigned to either the bone mineral or collagen matrix. In this bone specimen, we initially assigned these Raman bands to a bacterial pigment resembling xanthomonadin, a halogenated aryl-polyene. Raman identification of xanthomonadin pigments has been reported in plant-associated bacteria such as the *Xanthomonas* family, but never in human tissue.⁷ Microbiology tests revealed *Stenotrophomonas maltophilia* in the foot wound, which is similar in taxonomy to the *Xanthomonas* family and also produces a halogenated aryl-polyene.⁸

Later in the course of the study, we received a bone specimen from the Ann Arbor Veterans Affairs (VA) hospital pathology laboratory. This specimen had visible signs of contamination from a marking dye. Marking dyes are commonly used to orient the sample of fixed or fresh tissue, and a blue marking was used liberally on this VA specimen. Raman spectra of the VA specimen revealed the same pattern of sharp bands that was observed in the UM specimen. A pure component Raman spectrum of the

blue marking dye proved that the source of the unusual bands was the blue marking dye and not a bacterial pigment.

2 Materials and Methods

2.1 Bone Specimens

This ongoing study is being performed at UM and the Ann Arbor VA hospitals. Each study component was approved by the Institutional Review Board of the appropriate hospital. This study is approved by the Institutional Review Board of both hospitals. The UM sample was collected from a diabetic foot wound of the calcaneus where diabetic osteomyelitis was suspected after clinical examination. Three days prior to debridement of the wound, a large soft tissue defect was identified in the calcaneus by magnetic resonance imaging (MRI). The MRI data supported the initial suspicion of osteomyelitis. A bone biopsy was taken from the wound site using a sterile technique during clinical debridement, the typical clinical treatment for osteomyelitis. A first fragment of the bone biopsy was immediately separated and stored in a 10% formalin solution and later cultured for bacterial identification using standard microbiology techniques. The remainder of the biopsy was stored in a 1× phosphate buffered saline (PBS, Invitrogen, Grand Island, New York) with calcium and magnesium added. This PBS solution was enriched with 0.005% (w/v) sodium azide (Riedel de Haen, Seelze, Germany) and 0.1% (v/v) protease inhibitor cocktail (Sigma-Aldrich, St. Louis, Missouri) to prevent bacterial degradation. The bone biopsy was assessed for gross pathological appearance by the University of Michigan Pathology services, and a second small fragment (approximately 3 × 4 × 2 mm³) was separated from the biopsy by the pathology

Address all correspondence to: Blake J. Roessler, University of Michigan Medical School, Department of Internal Medicine, Division of Rheumatology, 3560 MSRB 2, 1150 W. Medical Center Drive, Ann Arbor, Michigan 48109-0688. Tel: +1-734-763-7949; Fax: (734)764-3596; E-mail: roessler@umich.edu

laboratory. The fragment prepared by pathology was examined by Raman microspectroscopy. The VA sample was collected from a toe amputation where diabetic osteomyelitis was confirmed. The bone specimen was immediately transferred to surgical pathology, where a blue tissue marking dye (Cancer Diagnostics Inc., Morrisville, North Carolina) was used to mark the orientation before the tissue was sectioned for the preparation of histology slides. Tissue marking dyes are commonly used by pathologists to maintain an orientation reference after sectioning the tissue, by adding a unique color to the known margins of a specimen. A section of the tissue near the amputation site was stored in enriched PBS at 4°C until examination by Raman microscopy.

2.2 Drop Deposition of Pathology Dyes

Thirteen tissue-marking dyes from two manufacturers (Cancer Diagnostics Inc., $n = 6$, and Bradley Products Inc., Bloomington, Minnesota, $n = 7$) were obtained from the VA pathology laboratory and examined without further preparation. Drop deposition was used to prepare dyes for Raman spectroscopy. A small volume ($< 100 \mu\text{l}$) of dye were deposited onto a gold-coated glass slide (EMF Corporation, Ithaca, New York) and allowed to dry in ambient conditions. Dried drops were examined by light microscopy and Raman microspectroscopy. Raman spectra were collected across the surface of the dried drop.

2.3 Raman Microspectroscopy

Bone fragments were examined by stereo microscopy and Raman microspectroscopy within a day of receipt. Dried drops were examined by Raman microspectroscopy. Low magnification images of bone fragments were collected using a Nikon

SMZ1000 stereo microscope (Nikon, Melville, New York). The near-infrared Raman microspectroscopy instrument was constructed in-house and is described in detail elsewhere.⁹ Laser intensity was $\sim 100 \text{ mW}$ at the sample using a $20\times/0.75 \text{ NA}$ Nikon S Fluor objective, resulting in a $100 \times 10 \mu\text{m}^2$ laser line with average power density of $1 \times 10^4 \text{ W/cm}^2$. After preprocessing, transects consisted of 126 spectra spaced at equidistant points along the line. Transects were imported into Matlab (version 2011a, The Math Works, Natick, Massachusetts) and corrected for image distortions, dark current and variations in the CCD efficiency using vendor-supplied and custom-written scripts.¹⁰ A mean spectrum was calculated from the transect, and the mean spectrum was baseline-corrected using the method described by Cao et al.¹¹

3 Results and Discussion

This paper represents the fourth case report in the past 30 years where *S. maltophilia* was reported in osteomyelitis, underscoring the scarcity of this bacterium in bone infections.¹² Raman analysis of the UM bone fragment yielded unusual Raman spectra in some locations and spectra consistent with normal bone composition in other locations, suggesting substantial compositional heterogeneity within the bone fragment. A spectrum from the UM specimen at a site of normal bone composition is shown in Fig. 1(a). At a few sites on the UM specimen, unusual bands that could not be assigned to bone were found [labeled with an asterisk in Fig. 1(b)]. At these sites, spectra also indicated unusual mineral and matrix composition.

Based on the literature reports and microbiology results, we initially hypothesized that the unusual bands were from a bacterial pigment. To our best knowledge, there are no Raman reports of the pigment in *S. maltophilia*, even though there is an FTIR spectroscopy study that included *S. maltophilia*.¹³

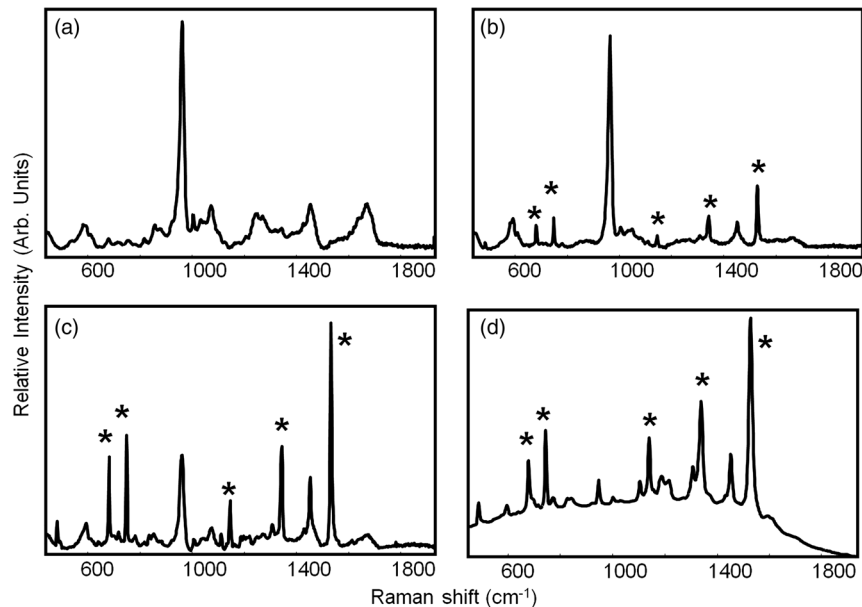


Fig. 1 Raman spectra from the University of Michigan (UM) human bone fragment affected by diabetic osteomyelitis revealed compositional heterogeneity of the tissue, even within a small $3 \times 4 \text{ mm}^2$ fragment. (a) Spectrum from a portion of the UM specimen representative of normal bone composition. Unusual bone composition and sharp bands at 679 , 749 , 1143 , 1339 , and 1526 cm^{-1} (marked with an asterisk) was observed in a few sections of the UM specimen (b). These unusual bands were not previously observed in bone Raman spectra and were initially assigned as a bacterial pigment. Unusual bands were again observed in spectra from a Veterans Affairs (VA) human bone fragment, seen in (c). Comparison of the bands seen in the UM and VA spectra with a pure component spectrum of blue marking dye (d) revealed that the source of the unusual bands was a blue marking dye and not a bacterial pigment. Bands at 679 , 749 , 1143 , 1339 , and 1526 cm^{-1} are marked with an asterisk in panels (b) to (d).

Bands at 1143 and 1526 cm^{-1} in the UM specimen were initially assigned to the pigment polyene. This assignment was based on a previous study of xanthomonadin, a pigment similar to the one found in *S. maltophilia*, showing strong bands at 1135 and 1531 cm^{-1} (Refs. 7 and 14). Bands at 678, 746, 1307, and 1339 cm^{-1} were assigned based on literature reports of biological pigments and substituted benzenes.^{15–18}

A spectrum from the VA specimen [Fig. 1(c)], which has been visibly contaminated with a blue marking dye, showed the same unusual bands [asterisk, Fig. 1(c)] that were observed in the UM specimen. We did not consider the possibility that the UM specimen had been contaminated because the specimen handling was observed by the primary investigators at all stages from collection to Raman analysis. Furthermore, visual inspection of the UM specimen, shown in Fig. 2(a), did not reveal any obvious discoloration. By contrast, the VA specimen was visibly contaminated with blue tissue-marking dye, shown in Fig. 2(b). After realizing that the pathology dyes may have contaminated the samples, we performed drop deposition/Raman spectroscopy to obtain pure component spectra of 13 commonly used pathology marking dyes. Raw data files of all the marking dyes are available in .ascii, .mat, or .spc file formats upon request.

For brevity, we present data of only the blue marking dye. A spectrum of the blue marking dye, shown in Fig. 1(d), contained bands that matched exactly with the unusual bands observed in the UM and VA specimens. Thus the unusual bands in those specimens arose from the blue marking dye and not a bacterial pigment. The blue marking dye likely has conjugation structure because of the presence of bands at 1143 and 1526 cm^{-1} . This poses two potential issues. The first is that these bands may overlap with aromatic ring, condensed ring, or polyene bands that are expected from carotenoids or other natural pigments in the ~ 1140 to 1150 cm^{-1} and 1520 to 1530 cm^{-1} regions. More importantly, the presence of resonance enhancement in the dye means that even trace amounts, invisible to the eye, will give a strong Raman spectrum.¹⁹ We suspect this was the case with the UM specimen and believe that it had been handled by tools with a trace amount of dye contaminant.

The bone Raman spectrum is dominated by contributions from the carbonated apatite mineral and collagen matrix. Except for the ring breathing mode of phenylalanine at $\sim 1003 \text{ cm}^{-1}$, sharp bands are normally not found in bone Raman spectra except for the occasional instance where residual blood is on the specimen. If sharp bands are found in a bone Raman

spectrum, they are easily recognized as abnormal. This was the case when we first observed unusual bands in the UM specimen, and we immediately recognized that these bands did not arise from bone. However, if the Raman spectrum of a specimen was expected to contain pigment bands, then it is possible that dye bands may be mistaken for a biological pigment.

4 Conclusions

Fresh tissue for spectroscopic analysis is routinely handled first by pathology laboratories. In our Raman spectroscopy study of bone in diabetic osteomyelitis, spectra were collected from bony tissue that would otherwise be discarded after the pathology laboratory collects an appropriate specimen. An unexpected finding was the observation of pigment-like bands in bone tissue collected from one UM patient and one VA patient. We were only able to determine that the unusual bands came from a pathology tissue-marking dye because the VA specimen had visibly been contaminated. The UM specimen did not have any visible evidence of contamination, but its Raman spectra clearly contained bands from the blue marking dye. The dye was only observed in 2 of 17 specimens and may have been overlooked in the UM specimen if fewer transects were taken. Thus it is possible that even vanishingly small amounts of contaminating tissue-marking dyes, invisible to the eye, may result a misinterpretation of the spectrum. Pathology investigation of tissue typically involves first fixing the tissue and then using various stains to identify features of interest. Trace contamination of a sample by a tissue-marking dye would have no effect on pathology results. However, resonance or even preresonance enhancement makes Raman spectroscopy extremely sensitive to the presence of some dyes. Investigators studying clinical tissue samples previously handled by a pathology lab should anticipate that trace dye contamination may be observed.

Acknowledgments

This work was supported by grant R21EB101026 from the National Institute of Biomedical Imaging and Bioengineering, NIH (BJR), a training grant T32AR007080 from National Institute of Arthritis and Musculoskeletal and Skin Diseases, NIH/NIAMS (KEW) and a career development grant as part of a CTSA grant UL1RR024986 from National Center for Research Resources, NIH/NCRR (KEW). The authors thank Kaiser Optical Systems for instrument support. We thank Dr. Crystal Holmes, Dr. Jeffrey Kozlow, and Jill Southwick as our clinical collaborators. Duane Newton from University of Michigan Health Systems clinical microbiology provided clinical isolates of *S. maltophilia* bacteria. UMHS Tissue Procurement Core, UMHS Comprehensive Cancer Center (Grant CA49652), and Dr. Steven Chensue and Lynn St. Dennis, VA Pathology, prepared bone specimens. Brad Clay and Dave Pincus from bioMérieux, Inc. provided helpful discussions on *S. maltophilia*.

References

1. S. Bohic et al., "Characterization of the trabecular rat bone mineral: effect of ovariectomy and bisphosphonate treatment," *Bone* **26**(4), 341–348 (2000).
2. K. A. Dehring et al., "Identifying chemical changes in subchondral bone taken from murine knee joints using Raman spectroscopy," *Appl. Spectrosc.* **60**(10), 1134–1141 (2006).
3. R. J. Lakshmi et al., "Osteoradionecrosis (ORN) of the mandible: a laser Raman spectroscopic study," *Appl. Spectrosc.* **57**(9), 1100–1116 (2003).

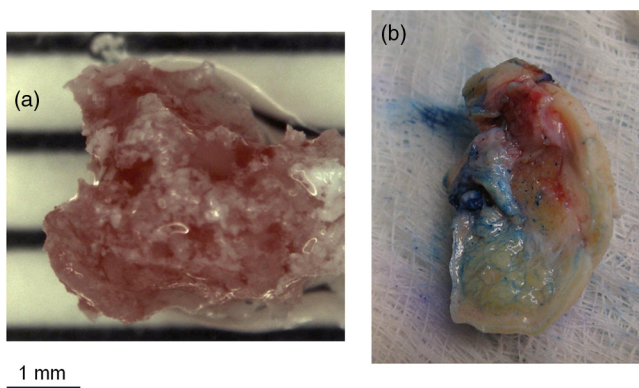


Fig. 2 Stereo microscopy images ($1\times$ magnification) of the UM and VA bone specimens. In the UM bone specimen, shown in (a), there was no visual evidence of contamination. By contrast, the VA specimen, shown in (b), was contaminated throughout with blue tissue marking dye.

4. X. Bi et al., "Characterization of bone quality in prostate cancer bone metastases using Raman spectroscopy," *Proc. SPIE*, **7548**, 75484L (2012).
5. K. A. Esmonde-White et al., "Raman spectroscopy of bone metastasis," *Proc. SPIE* **8207**, 82076P (2012).
6. J. R. Maher et al., "Raman spectroscopy detects deterioration in biomechanical properties of bone in a glucocorticoid-treated mouse model of rheumatoid arthritis," *J. Biomed. Opt.* **16**(8), 087012 (2011).
7. M. L. Paret et al., "Biochemical characterization of gram-positive and gram-negative plant-associated bacteria with micro-Raman spectroscopy," *Appl. Spectrosc.* **64**(4), 433–441 (2010).
8. C. L. Jenkins and M. P. Starr, "Formation of halogenated aryl-polyene (Xanthomonadin) pigments by the type and other yellow-pigmented strains of *Xanthomonas maltophilia*," *Ann. Inst. Pasteur Microbiol.* **136**(3), 257–264 (1985).
9. K. A. Esmonde-White et al., "Fiber-optic Raman spectroscopy of joint tissues," *Analyst* **136**(8), 1675–1685 (2011).
10. F. W. L. Esmonde-White, K. A. Esmonde-White, and M. D. Morris, "Minor distortions with major consequences: correcting distortions in imaging spectrographs," *Appl. Spectrosc.* **65**(1), 85–98 (2011).
11. A. Cao et al., "A robust method for automated background subtraction of tissue fluorescence," *J. Raman Spectrosc.* **38**(9), 1199–1205 (2007).
12. W. A. Agger et al., "Wounds caused by corn-harvesting machines: an unusual source of infection due to gram-negative bacilli," *Rev. Infect. Dis.* **8**(6), 927–931 (1986).
13. A. Bosch et al., "Fourier transform infrared spectroscopy for rapid identification of nonfermenting gram-negative bacteria isolated from sputum samples from cystic fibrosis patients," *J. Clin. Microbiol.* **46**(8), 2535–2546 (2008).
14. N. J. Palleroni and J. F. Bradbury, "Stenotrophomonas, a new bacterial genus for *Xanthomonas maltophilia* (Hugh 1980) Swings et al. 1983," *Int. J. Syst. Bacteriol.* **43**(3), 606–609 (1993).
15. S. Jorge-Villar et al., "Raman and SEM analysis of a biocolonised hot spring travertine terrace in Svalbard, Norway," *Geochem. Trans.* **8**(1), 8 (2007).
16. H. Hayashi, T. Noguchi, and M. Tasumi, "Studies on the interrelationship among the intensity of a Raman marker band of carotenoids, polyene chain structure, and efficiency of the energy transfer from carotenoids to bacteriochlorophyll in photosynthetic bacteria," *Photochem. Photobiol.* **49**(3), 337–343 (1989).
17. H. Schulz, M. Baranska, and R. Baranski, "Potential of NIR-FT-Raman spectroscopy in natural carotenoid analysis," *Biopolymers* **77**(4), 212–221 (2005).
18. D. Lin Vien et al., *Handbook of Infrared and Raman Characteristic Frequencies of Organic Molecules*, Academic Press, San Diego (1991).
19. E. Smith and G. Dent, *Modern Raman Spectroscopy—A Practical Approach*, John Wiley & Sons, Chichester, West Sussex (2005).